Image Thresholding by Minimizing Tsallis Divergence Measure

Fangyan Nie, Xiaolin Wang, Shuanghui Yu and Zhifei Liao

College of Computer Science and Technology,
Hunan University of Arts and Science, Changde 415000, China
niefyan@163.com

Abstract

This paper presents a novel image segmentation method that performs histogram thresholding based on the conception of Tsallis generalized divergence. Firstly, to fit the image segmentation task, the original formula of Tsallis divergence was simplified, and then the symmetrical version was constructed. After that, the criterion of divergence sum of the objective and background between original and thresholded image was set up based on the symmetrical version of the Tsallis divergence. The optimal threshold obtained by minimizing the criterion of divergence sum. Finally, the proposed method was tested on different gray level images, and the performance was evaluated using uniformity measure, shape measure, and CPU run time. Experimental results indicate the effectiveness of the proposed method.

Keywords: image segmentation; histogram thresholding; Tsallis generalized divergence

1. Introduction

In many scenarios, image segmentation is the foundation of image processing task, and it is one of the important contents of computer vision research [1]. In recent decades, a lot of approaches for image segmentation have been proposed by many researchers, and these methods have been successfully used in image analysis fields, such as medical image analysis [2], SAR image analysis [3], infrared image processing [4], etc. Among these methods, the thresholding approach is one the most popular technology be used because of its simplicity and effectiveness [5]. The entropy-based method is the famous technology for image segmentation in histogram thresholding methods [5-7]. The first entropy-based method is proposed by Pun [8], and then another entropy-based approach is proposed by Kapur et al. through correcting the insufficiency in the Pun's method [9]. In recent years, with the development of nonextensive statistical mechanics, the nonextensive entropy proposed by Tsallis (also called Tsallis entropy) has obtained application successfully in many physical fields [10]. In image segmentation, the first method used Tsallis entropy was proposed by Port de Albuquerque *et al.* [11], and then some improved methods were proposed in several literatures [12-14].

Among image thresholding methods, the cross entropy based is a powerful branch. In many literatures the cross entropy is also known as relative entropy, Kullback-Leibler information, divergence, etc. When the cross entropy is used in image segmentation, it was as a distance measure usually, so we prefer to call it divergence in this paper. The first threholding method based cross entropy was presented by Li and Lee [15], and Brink and Pendock demonstrates the relationship between cross entropy based thresholding method and Otsu measure later [16]. Pal proposed another cross entropy thresholding method based on Poisson distribution [17]. Kittler and Illingworth proposed a minimum error thresholding method based on Gaussian mixture distribution [18], and Fan and Xie proved that this method is

also a relative entropy method later [19]. Tsallis puts forward a concept of generalized divergence in 1998 (also known as Tsallis divergence) [20]. Considering the cross entropy meaning exist in Tsallis divergence, Tang et al. proposed a minimum Tsallis cross entropy thresholding method based on mixture uniform distribution, and claim that their method achieved better results on segmentation efficiency and time performance [21]. Based on Tsallis generalized divergence, we put forward a new image thresholding method in this paper. For evaluating the performance of new method, the new method is compared with several traditional cross entropy methods and Tang's method. The experimental results show the effectiveness of proposed method for image segmentation.

2. Thresholding Principle based on Tsallis Divergence

2.1. Tsallis Divergence

Assuming that $\Delta = \{(x_1, x_2, \cdots, x_n) \mid 0 \le x_i \le 1, \sum_1^n x_i = 1\}$, $\boldsymbol{P}, \boldsymbol{Q} \in \Delta$, then the Tsallis divergence between probability vector $\boldsymbol{P}$, $\boldsymbol{Q}$ can be defined by following equation [20].

$$D_q(\boldsymbol{P} \mid \boldsymbol{Q}) = -\sum_{i=1}^{n} p_i \ln_q(q_i / p_i) \tag{1}$$

Where $q \ge 0$ and $q \ne 1$, $\ln_q(\cdot)$ denote the q-logarithmic function, it is defined as

$$\ln_q(x) = (x^{1-q} - 1)/(1-q) \tag{2}$$

Obviously, when $q \rightarrow 1$, Tsallis divergence converge to the classical divergence forms, *i.e.*

$$\lim_{q \rightarrow 1} D_q(\boldsymbol{P} \mid \boldsymbol{Q}) = D_1(\boldsymbol{P} \mid \boldsymbol{Q}) = \sum_{i=1}^{n} p_i \ln(p_i / q_i) \tag{3}$$

2.2. Image Thresholding

Assuming that $\boldsymbol{I}$ is an image with size $M \times N$ and L grayscale, $\boldsymbol{I} = \{f(x,y) \mid x \in \{1,2,\cdots,M\}, y \in \{1,2,\cdots,N\}\}$, $f(x,y)$ denote the pixel value at (x,y), $f(x,y) \in \boldsymbol{G} = \{0,1,\cdots,L\text{-}1\}$. In addition, assuming that the image histogram is $\boldsymbol{H} = \{h_0, h_1, \cdots, h_{L-1}\}$, h_i denote the frequency of grayscale i. The normalized histogram can be denoted by $\boldsymbol{P} = \{p_0, p_1, \cdots, p_{L-1}\}$, where $p_i = h_i/(M \times N)$. For 8-bit grayscale digital image, $L = 256$.

Assuming that t is a threshold when thresholding method is used for image segmentation, the image is divided into two parts by t, the pixels belong to $\{0,1,\cdots,t\}$ represent the background (or foreground), and the other pixels belong to $\{t+1,t+2,\cdots,L\text{-}1\}$ denote the foreground (or background). According to the form of equation (3), Li and Lee proposed a cross entropy based thresholding method, i.e.

$$D(t) = \sum_{i=0}^{t} i h_i \log(i/\mu_1(t)) + \sum_{i=t+1}^{L-1} i h_i \log(i/\mu_2(t)) \tag{4}$$

where

$$\mu_1(t) = \sum_{i=0}^{t} (i h_i) \left/ \sum_{i=0}^{t} h_i \right. \tag{5}$$

$$\mu_2(t) = \sum_{i=t+1}^{L-1} (i h_i) \left/ \sum_{i=t+1}^{L-1} h_i \right. \tag{6}$$

Based on the form of equation (1), Tang et al. presented a minimum Tsallis cross entropy thresholding method using mixture uniform distribution [21]. In their method the normalized histogram $\boldsymbol{P} = \{p_0, p_1, \cdots, p_{L-1}\}$ is used to denote the probability distribution of

original image grayscale, the probability distribution of grayscale of thresholded image is represented by uniform distribution, i.e.

$$q_i = \begin{cases} P_O/(t+1); & 0 \le i \le t \\ P_b/(L-t-1); & t < i \le L-1 \end{cases} \tag{7}$$

where $P_O = \sum_{i=0}^{t} p_i$, $P_b = 1 - P_o$.

Sometimes, the difference between the probability vectors cannot be well measured by the classical divergence. So the good segmented results can not be obtained through the thresholding method based on equation (4), even bring error segmentation in this case. The method based on Tsallis cross entropy proposed by Tang et al. improve the segmentation performance compared with classical cross entropy based thresholding method. However, the authors use the uniform distribution to depict the grayscale probability distribution of thresholded image. The image is a complex system, so this depiction is clearly not appropriate. For obtaining better segmented result through thresholding method based on the principle of Tsallis divergence, we presented a new approach for image segmentation in this paper. Firstly, substituting the Equation (2) into Equation (1), and then simplified, we obtain Equation (8) as follows.

$$\begin{aligned} D_q(\boldsymbol{P} \mid \boldsymbol{Q}) &= -\sum_{i=1}^{n} p_i \ln_q \frac{q_i}{p_i} \\ &= -\sum_{i=1}^{n} p_i \frac{(q_i/p_i)^{1-q} - 1}{1-q} \\ &= \frac{1}{q-1}\left[\sum_{i=1}^{n} q_i (p_i/q_i)^q - 1\right] \end{aligned} \tag{8}$$

In general, $D_q(\boldsymbol{P}|\boldsymbol{Q})$ is asymmetrical, the symmetric version of equation (8) can be defined as

$$\begin{aligned} J_q &= D_q(\boldsymbol{P} \mid \boldsymbol{Q}) + D_q(\boldsymbol{Q} \mid \boldsymbol{P}) \\ &= \frac{1}{q-1}\left[\sum_{i=1}^{n} q_i \left(\frac{p_i}{q_i}\right)^q + \sum_{i=1}^{n} p_i \left(\frac{q_i}{p_i}\right)^q - 2\right] \end{aligned} \tag{9}$$

i. e.

$$J_q = \frac{1}{q-1}\left\{\sum_{i=1}^{n}\left[p_i\left(\frac{q_i}{p_i}\right)^q + q_i\left(\frac{p_i}{q_i}\right)^q\right] - 2\right\} \tag{10}$$

For the sake of convenience, according to Equation (10) we let

$$\Lambda_i^b(t) = ih_i\left(\mu_1(t)/i\right)^q + \mu_1(t)h_i\left(i/\mu_1(t)\right)^q \tag{11}$$

$$\Lambda_i^o(t) = ih_i\left(\mu_2(t)/i\right)^q + \mu_2(t)h_i\left(i/\mu_2(t)\right)^q \tag{12}$$

then substituting Equation (11) and (12) into (10), we can obtain the Tsallis divergences of the foreground and background of thresholded image, i.e.

$$J_q^b(t) = \frac{1}{q-1}\left(\sum_{i=0}^{t} \Lambda_i^b(t) - 2\right) \tag{13}$$

$$J_q^o(t) = \frac{1}{q-1}\left(\sum_{i=t+1}^{L-1} \Lambda_i^o(t) - 2\right) \tag{14}$$

The total Tsallis divergence of threshold image can be defined by

$$J_q(t) = J_q^b(t) + J_q^o(t) \tag{15}$$

To get the optimal threshold for image segmentation, the Equation (15) is minimized, *i.e.*

$$t^* = \arg \min_{t \in G} J_q(t) \qquad (16)$$

Where t^* denotes the optimal threshold, after that the image can be segmented by

$$\bar{f}(x,y) = \begin{cases} 0; 0 \le f(x,y) \le t^* \\ 1; t^* < f(x,y) \le L-1 \end{cases} \qquad (17)$$

Where $\bar{f}(x,y)$ denotes the thresholder image, $f(x,y)$ denotes the pixel value at (x,y) in original image.

3. Experimental Results and Performance Evaluation

Considering the comparability in the process of experiment, the minimum error threholding (MET) [18] method proposed by Kittler and Illingworth, the minimum cross entropy (MCE) [15] thresholding method proposed by Li and Lee, and the method proposed by Tang *et al.* based on Tsallis cross entropy (Tang *et al.'s* method) [21] are selected for comparing with the method proposed in this paper. The selected methods are the most classic methods for image thresholding based on the concept of divergence, so they are selected for comparing with the proposed method. The all methods are programmed with Matlab language, and run on a computer with Pentium(R) 4 CPU 2.66GHz, 2GB RAM, and the operating system is Microsoft Windows XP Professional.

In order to assess the performance of each method adequately, the experiments are carried out on a large number of images. Due to the limit of space, 3 classical images used for assessing segmentation performance of thresholding method in many case, and an infrared human image taken by a forward-looking infrared thermal imaging instrument Thermovision A40M are selected for demonstrating the performance of each method in this paper. The four image are show in Figure 1, and they are named "bacteria", "blood1", "lena", and "pedestrian". The histograms of the 4 images are show in Figure 1 also. As can be seen from Figure 1, the histograms of the 4 images are dense or sparse, and the shapes of the 4 histogram are different, they are bimodal distribution, or multimodal distribution.
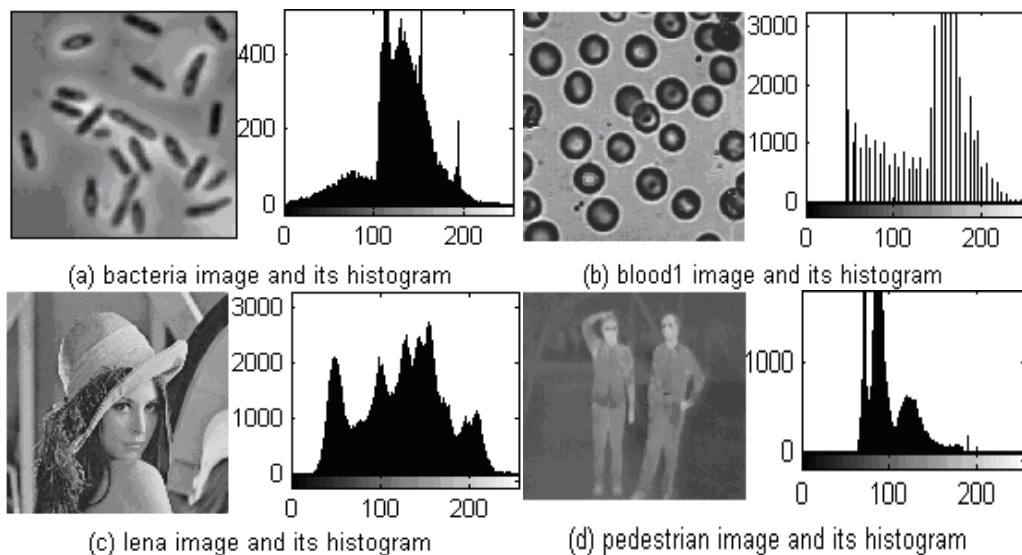
3.1. Experimental Results and Analysis

Unless otherwise stated, the parameter q of the proposed method in this paper is set as 2. According to the original paper of Tang et al., the parameter q of Tang et al.'s method is set as 0.5. Table 1 lists the optimal thresholds obtained by four methods on four test images. Figures 2-5 show the thresholded images using four methods on four tested images respectively.
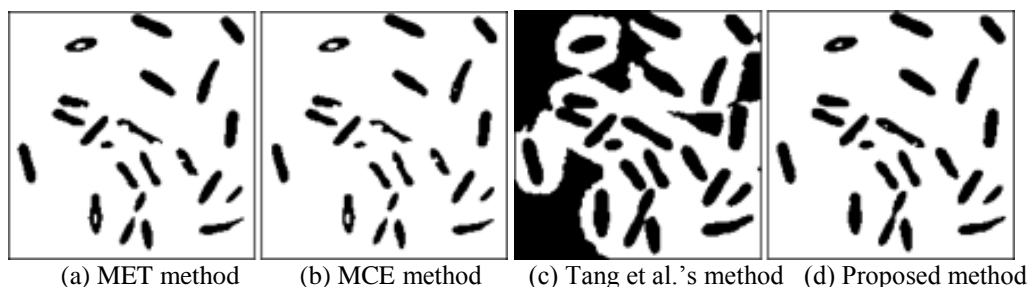
As we can see from Figure 1 and Table 1, the thresholds obtained by the proposed method are mostly located at the near the valley of image histogram except the "lena" image which distribution of histogram is obvious multimodal. While the thresholds obtained by MET and Tang method, are deviated from the valley of histogram visibly. The optimal thresholds obtained by MCE method are most similar to the thresholds that obtained by the proposed method. But by watching the data that in Figure 1 and Table 1 carefully, it can be seen that there are subtle differences between the results obtained by the proposed method and MCE method. The optimal thresholds obtained by the proposed method are more accurately near the valley of image histograms. In addition, from Figure 4 we can see that the ideal segmentation result is get when the optimal threshold obtained by the proposed method is used to segment the "lena" image.

Table 1. Comparison of Optimal Thresholds Obtained by Different Methods on Test Images

Image	MET	MCE	Tang et al.'s method	Proposed method
bacteria	88	85	124	99
blood1	48	96	46	101
lena	75	107	127	106
pedestrian	103	105	94	105

(a) bacteria image and its histogram   (b) blood1 image and its histogram

(c) lena image and its histogram   (d) pedestrian image and its histogram

Figure 1. Test Images and Their Histograms

(a) MET method   (b) MCE method   (c) Tang et al.'s method   (d) Proposed method

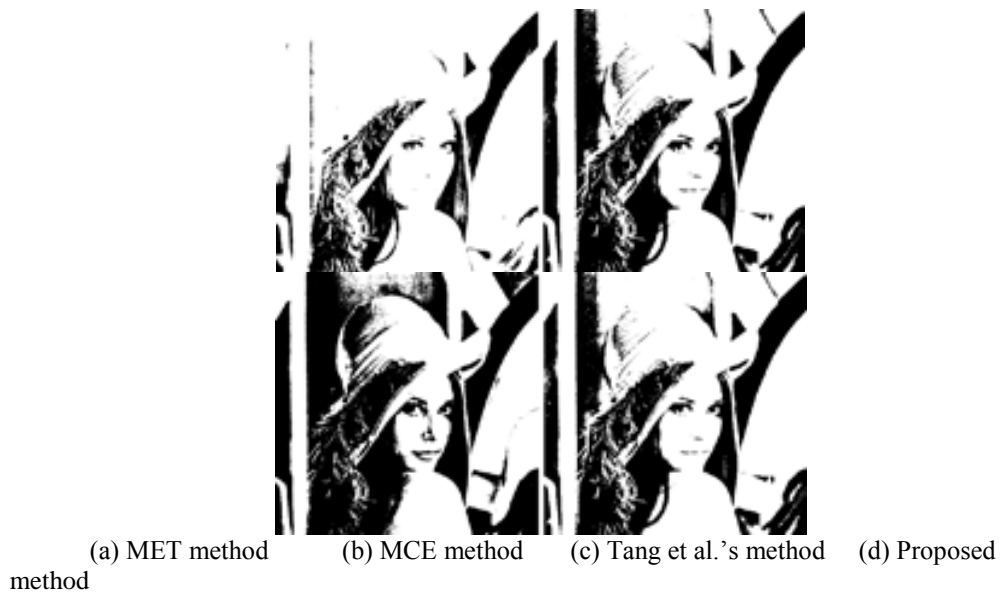**Figure 2. Threshold Segmentation Results of "bacteria" Image**

For "bacteria" image, from Figure 2 we can see that the bacteria individual are separated from background integrally when the threshold obtained by the proposed method is used to threholding "bacteria" image, and the isolated bacteria individual are full also. While for the results obtained by MET and MCE method, some isolated bacteria individual are fractured, and become incomplete. For the method proposed by Tang *et al.*, the bacteria individual are basically barely been separated from the background.

Figure 3 shows the segmented results of "blood1" image by different methods. From Figure 3, we can see that the segmented results obtained by MCE and the proposed method are good, and the blood cells separated from background are distinguished. While the majority of blood-cells in segmented result images obtained by MET and Tang *et al.'s* method become splintered and incomplete.

(a) MET method   (b) MCE method   (c) Tang et al.'s method   (d) Proposed method
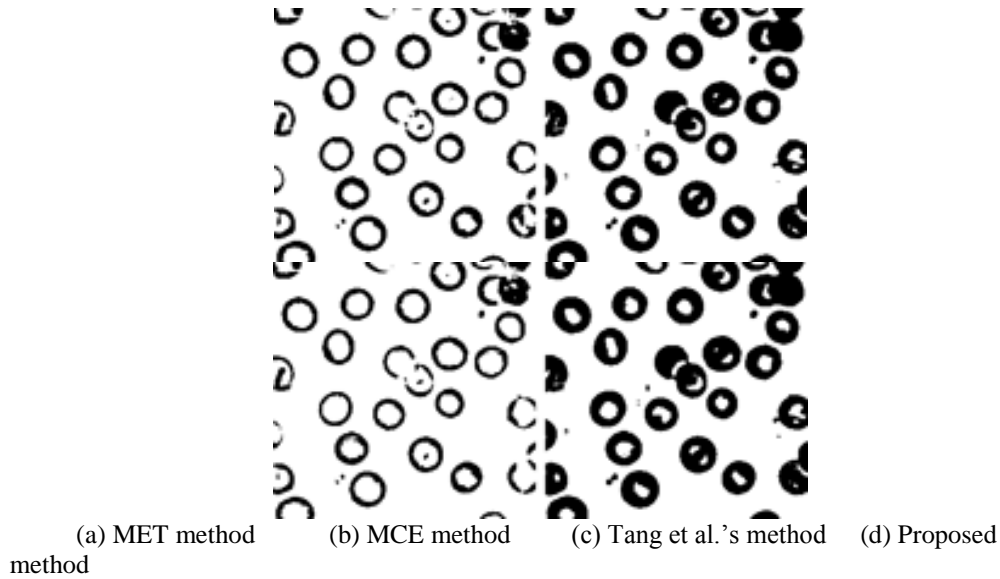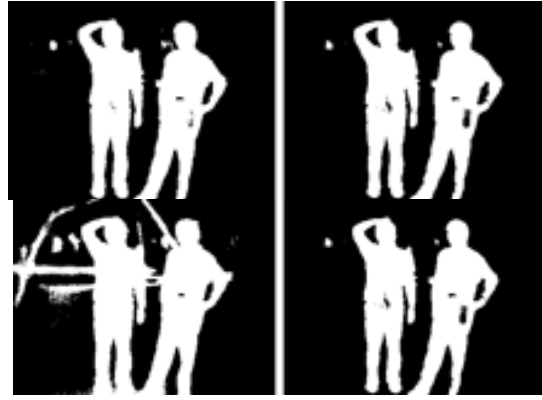
Figure 3. Threshold Segmentation Results of "blood1" Image

Figure 4 shows the segmented results of "lena" image by different methods. From Figure 4 it can be seen that the details of portrait in the thresholded images obtained by MCE and the proposed method are clearly and rich, the edge is smooth. The result obtained by MET method seems a bit over-segmentation and the result obtained by Tang *et al.'s* method seems under-segmentation from the vision.

(a) MET method   (b) MCE method   (c) Tang et al.'s method   (d) Proposed method

Figure 4. Threshold Segmentation Results of "lena" Image

Figure 5 shows the segmented results of "pedestrian" image by different methods. From Figure 5 we can see that the result obtained by Tang *et al.'s* method is the worst among the results obtained by four methods, there are more background interference pixels exist in the segmented result. The pedestrian targets in "pedestrian" image are separated from background well by the MET, MCE and the proposed method.

(a) MET method   (b) MCE method   (c) Tang et al.'s method   (d) Proposed method

Figure 5. Threshold Segmentation Results of "pedestrian" Image

By comparing the segmented results getting from different methods, it can be seen that the target of image can be separated from background well through the proposed method in this paper. Besides the abovementioned images, the experiments on a large number of test images can also get the same conclusion.

3.2. Performance Evaluation

In order to avoid error by visual analysis, and from more objective perspectives to evaluate the performance of various methods, the uniformity measure (UM) [22] and shape measure (SM) [23] that usually as the objective evaluation criteria for evaluating the performance of different image segmentation methods are selected to evaluate the proposed method. For a given threshold value t, the arithmetic expressions of UM and SM can be defined as follows equations.

$$UM = 1 - \frac{1}{C}\left[\sigma_B^2(t) + \sigma_F^2(t)\right] \tag{18}$$

The uniform measure is usually used for the measurement of the homogeneity of the object in the test images. Where, C is a normalization factor, B and F denote the background and foreground of image, respectively. Assume that $X=B$ or F, then $\sigma_X^2(t)$ can be defined by

$$\sigma_X^2(t) = \sum_{(x,y)\in R_X}\left[\left(f(x,y) - \mu_X\right)^2\right] \tag{19}$$

Where R_X denotes the segmented region X, $f(x,y)$ denotes the gray level of the pixel (x,y), μ_X denotes the average value of gray level value of pixels in region R_X, it is defined as

$$\mu_X = \frac{1}{N_X}\sum_{(x,y)\in R_X} f(x,y) \tag{20}$$

Where, N_X denotes the number of pixels in R_X.

The shape measure is usually used for the measurement of the shape of the object in the test images. It can be defined as

$$SM = \frac{1}{C}\sum_{(x,y)}\text{sgn}\left(f(x,y) - \overline{f_{N(x,y)}}\right)\cdot \Delta(x,y)\cdot\text{sgn}\left(f(x,y) - t\right) \tag{21}$$

Where $\overline{f_{N(x,y)}}$ is the average gray value in the neighborhood $N(x,y)$, C is a normalization factor, and

$$\mathrm{sgn}(x) = \begin{cases} +1 & if \ x \geq 0 \\ -1 & if \ x < 0 \end{cases} \tag{22}$$

$$\Delta(x,y) = \left[\sum_{d=1}^{4} D_d^2 + \sqrt{2} D_1(D_3 + D_4) - \sqrt{2} D_2(D_3 - D_4) \right]^{\frac{1}{2}} \tag{23}$$

Where $D_1 = f(x+1,y) - f(x-1,y)$, $D_2 = f(x,y-1) - f(x,y+1)$, $D_3 = f(x+1,y+1) - f(x-1,y-1)$, and $D_4 = f(x+1,y-1) - f(x-1,y+1)$.

UM and *SM* are the best-known objective evaluation criteria for evaluating the performance of image segmentation, and many literatures use the two criteria to judge the merits of the image segmentation methods [5,6,24].

Using the normalization factor *C*, the value of the *UM* and *SM* between 0 and 1. For a given threshold value *t*, the higher the value of *UM* and *SM*, the better the performance of segmentation algorithms. In this paper, the normalization factor *C* is defined as $C = (f_{max} - f_{min})^2$, where the f_{max} and f_{min} denote the maximum and minimum of pixels in the test images, respectively.

Using both two measures, the threshold value obtained according to each method abovementioned are evaluated. Table 2 and 3 show the results of this evaluation.

Table 2. The Performance Comparison on UM Measure for Different Methods

Image	MET	MCE	Tang et al.'s method	Proposed method
bacteria	0.9784	0.9782	0.9762	**0.9787**
blood1	0.9469	0.9821	0.9373	**0.9830**
lena	0.9574	**0.9706**	0.9702	0.9704
pedestrian	0.9834	0.9836	0.9785	**0.9836**

From Table 2, it can be seen that except "lena" image, the UM values for the thresholds obtained by the proposed method in this paper are bigger than that of other methods. The UM values for the Tang et al's method is lower than that of other methods.

Table 3. The Performance Comparison on SM Measure for Different Methods

Image	MET	MCE	Tang et al.'s method	Proposed method
bacteria	0.8773	0.8546	0.8277	**0.9698**
blood1	0.2864	0.9199	0.0517	**0.9479**
lena	0.8428	0.9894	0.8922	**0.9920**
pedestrian	0.8532	0.8980	0.6457	**0.8980**

From Table 3, we can see that the SM values obtained by the proposed methods are higher than that of other methods on all test images. The maximum of the SM for the optimal threshold obtained by the proposed method is 0.9920, it is pretty close to 1. While for the Tang et al's method, the SM values obtained this method are all lower than that of other methods, the minimum obtained by Tang et al's method is 0.0517.

The analysis results from Table 2 and 3 are consistent with results from the visual analysis on test images, it also reveal that the proposed method can obtained good segmentation result when the proposed method is used to image thresholding.

In many image processing task, the time-cost is a very important index for evaluating the performance of algorithm. The authors of Tang et al's method claim that the time-cost is less. For comparing the time performance, we test the CPU run time of all methods on test images. Table 4 shows the results.

Table 4. Time Performance Comparison on Test Images for Different Methods (Unit: millisecond)

Image	MET	MCE	Tang et al.'s method	Proposed method
bacteria	0.0940	0.0470	0.0620	**0.0470**
blood1	0.0940	0.0470	0.0930	**0.0470**
lena	0.0940	0.0630	0.0780	**0.0620**
pedestrian	0.0780	**0.0320**	0.0470	0.0460

From Table 4, we can see that the time-costs for the proposed method are equal to or less than that of other methods except "pedestrian" image. For 8-bits gray levels image, the CPU run time of the proposed method is 50 milliseconds approximately.

5. Conclusion

Several histogram thresholding methods are presented by lot researchers based on the conception of divergence of information theory in recent years. In this paper, by simplifying and deforming, we proposed a new and effective image thresholding segmentation approach based on Tsallis generalized divergence. The experimental results verify that the good segmentation results can be obtained when an appropriate parameter value of Tsallis divergence index q is selected for image thresholding. Based on two best-known objective evaluation criteria for evaluating the performance of image segmentation, i.e. uniformity measure and shape measure, the higher values can be obtained by the proposed method compared with several thresholding methods based on the classical divergence conception. For example, the UM values is greater than 0.9, and the highest value of SM can reach more than 0.99 on test images. The results on UM and SM also illustrate the effective of the proposed method. On the CPU time consumption, for 8-bits gray level image, the total run time of the proposed method is approximately 50 milliseconds. So for time performance, the proposed method satisfies the real-time requirement for many image processing tasks. In addition, the parameter q as an adjustable parameter, it may provide a possibility for the proposed method to fit the different image segmentation tasks.

Acknowledgements

References

[1] I. A. Yusoff, N. A. Mat and K. Hasikin, "Automated two-dimensional K-means clustering algorithm for unsupervised image segmentation", Computers & Electrical Engineering, vol. 39, no. 3, **(2013)**, pp. 907-917.

[2] F. A. M. Cappabianco, A. X. Falcão, C. L. Yasuda and J. K. Udupa, "Brain tissue MR-image segmentation via optimum-path forest clustering", Computer Vision and Image Understanding, vol. 116, no. 10, **(2012)**, pp. 1047-1059.

[3] R. C. Marques, F. N. Medeiros and J. Santos Nobre, "SAR image segmentation based on level set approach and GºA model", IEEE Transactions on Pattern Analysis and Machine Intelligence, vol. 34, no. 10, **(2012)**, pp. 2046-2057.

[4] D. S. Kim and K. H. Lee, "Segment-based region of interest generation for pedestrian detection in far-infrared images", Infrared Physics & Technology, vol. 61, **(2013)**, pp. 120-128.

[5] M. Sezgin and B. Sankur, "Survey over image thresholding techniques and quantitative performance evaluation", Journal of Electronic Imaging, vol. 13, no. 1, **(2004)**, pp. 146-165.

[6] F. Nie F, C. Gao, Y. Guo and M. Gan, "Two-dimensional minimum local cross-entropy thresholding based on co-occurrence matrix", Computers & Electrical Engineering, vol. 37, no. 5, **(2011)**, pp. 757-767.

[7] A. Yimit, Y. Hagihara, T. Miyoshi and Y. Hagihara, "2-D direction histogram based entropic thresholding", Neurocomputing, vol. 120, **(2013)**, pp. 287-297.

[8] T. Pun, "A new method for grey-level picture thresholding using the entropy of the histogram", Signal Processing, vol. 2, no. 3, **(1980)**, pp. 223-237.

[9] J. N. Kapur, P. K. Sahoo and A.K.C. Wong, "A new method for gray-level picture thresholding using the entropy of the histogram", Computer Vision, Graphics, and Image Processing, vol. 29, no. 3, **(1985)**, pp. 273-285.

[10] C. Tsallis, "Possible generalization of Boltzmann-Gibbs statistics", Journal of Statistical Physics, vol. 52, no. 1-2, **(1988)**, pp. 479-487.

[11] M. Portes de Albuquerque, I. A. Esquef and A. R. Gesualdi Mello, "Image thresholding using Tsallis entropy", Pattern Recognition Letters, vol. 25, no. 9, **(2004)**, pp. 1059-1065.

[12] P. K. Sahoo and G. Arora, "Image thresholding using two-dimensional Tsallis-Havrda-Charvat entropy", Pattern Recognition Letters, vol. 27, no.6, **(2006)**, pp. 520-528.

[13] Q. Lin and C. Ou, "Tsallis entropy and the long-range correlation in image thresholding", Signal Processing, vol. 92, no. 12, **(2012)**, pp. 2931-2939.

[14] P. S. Rodrigues and G.A. Giraldi, "Improving the non-extensive medical image segmentation based on Tsallis entropy", Pattern Analysis and Applications, vol. 14, no.4, **(2011)**, pp. 369-379.

[15] C. H. Li and C. K. Lee, "Minimum cross entropy thresholding", Pattern Recognition, vol. 26, no. 4, **(1993)**, pp. 617-625.

[16] A. D. Brink and N. E. Pendock, "Minimum cross-entropy threshold selection", Pattern Recognition, vol. 29, no. 1, **(1996)**, pp. 179-188.

[17] N. R. Pal, "On minimum cross-entropy thresholding", Pattern Recognition, vol. 29, no. 4, **(1996)**, pp. 575-580.

[18] J. Kittler and J. Illingworth, "Minimum error thresholding", Pattern Recognition, vol. 19, no. 1, **(1986)**, pp. 41-47.

[19] J. L. Fan and W. X. Xie, "Minimum error thresholding: a note", Pattern Recognition Letters, vol. 18, no. 8, **(1997)**, pp. 705-709.

[20] C. Tsallis, "Generalized entropy-based criterion for consistent testing", Physical Review E, vol. 58, no. 2, **(1998)**, pp. 1442-1445.

[21] Y. Tang, Q. Di, X. Guan and F. Liu, "Method for thresholding image segmentation based on minimum Tsallis-cross entropy", Chinese Journal of Scientific Instrument, vol. 29, no. 9, **(2008)**, pp. 1968-1872.

[22] M. D. Levine and A. M. Nazif, "Dynamic measurement of computer generated image segmentation", IEEE Transactions on Pattern Analysis and Intelligence, vol. PAMI-7, no. 2, **(1985)**, pp. 155-164.

[23] P. K. Sahoo, S. Soltani and A. K. C. Wong, "A survey of thresholding techniques", Computer Vision, Graphics, and Image Processing, vol. 41, no. 2, **(1988)**, pp. 233-260.

[24] C. I. Chang, Y. Du, J. Wang, S.M. Guo and P.D. Thouin, "Survey and comparative analysis of entropy and relative entropy thresholding techniques", IEE Proceedings - Image and Signal Processing, vol. 153, no. 6, **(2006)**, pp. 837-850.

Author

Fangyan Nie, he was born in Hunan province, China in 1977. He graduated from National University of Defense Technology, China in 1999. He received his M.S. degree in Computer Science and Technology from Guizhou University, China in 2005 and the Ph.D. degree in Instrument Science and technology from Chongqing University, China in 2010, respectively. Now he is an associate professor in the College of Computer Science and Technology, Hunan University of Arts and Science. His current research interests include information acquisition and processing, image processing and pattern recognition.